Poly(ethylene-alt-propylene)–poly(ethylene oxide) diblock copolymer micelles: a colloidal model system with *tunable softness*

2004 J. Phys.: Condens. Matter 16 S3821

(http://iopscience.iop.org/0953-8984/16/38/004)

INSTITUTE OF PHYSICS PUBLISHING JOURNAL OF PHYSICS: CONDENSED MATTER

J. Phys.: Condens. Matter **16** (2004) S3821–S3834 PII: S0953-8984(04)79835-5

Poly(ethylene-alt-propylene)–poly(ethylene oxide) diblock copolymer micelles: a colloidal model system with *tunable softness*

J Stellbrink[1], **G Rother, M Laurati, R Lund, L Willner and D Richter**

Institut für Festkörperforschung FZ Jülich, D-52425 Jülich, Germany

E-mail: j.stellbrink@fz-juelich.de

Received 26 April 2004
Published 10 September 2004
Online at stacks.iop.org/JPhysCM/16/S3821
doi:10.1088/0953-8984/16/38/004

Abstract

Kinetically frozen micelles formed by the amphiphilic diblock copolymer poly(ethylene-alt-propylene)–poly(ethylene oxide) (PEP–PEO) are proposed as a new model system for soft colloids. In this context soft is used with a twofold meaning: the *intra*particle softness, i.e. the molecular architecture of an individual micelle, as well as the *inter*particle softness, i.e. the effective potential for micellar interactions. Both contributions can be precisely adjusted from hard sphere-like to *ultrasoft* (star-like) by changing the diblock copolymer composition and/or interfacial tension, as shown by small angle neutron scattering in combination with contrast variation techniques.

Depending on the degree of softness, PEP–PEO micellar solutions respond variably to the application of external shear fields. In particular, in the star-like regime solutions are already extremely sensitive at low shear rates. Therefore these micelles are an excellent starting point for a comprehensive study on the relation between softness and non-equilibrium phase behaviour in colloidal systems.

(Some figures in this article are in colour only in the electronic version)

1. Introduction

The term soft colloid covers a broad range of particles from nearly all scientific fields starting from physics or chemistry and going over materials science to biology. The best known examples are probably charge-stabilized colloids used in physics as a model system for understanding fundamental laws of particle interactions [1, 2]. But also so-called hairy colloids [3, 4], i.e. colloidal particles coated with long polymer chains (the 'hairs'), or diblock

[1] Author to whom any correspondence should be addressed.

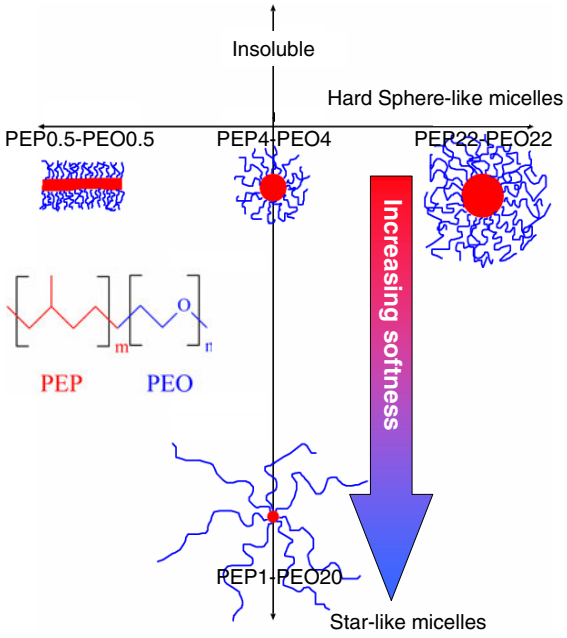

Figure 1. A sketch of the accessible micellar architectures by the use of PEP–PEO diblock copolymers.

copolymer micelles formed in a selective solvent [5], as well as microemulsions or protein aggregates and even whole cells can be regarded as soft colloids [6]. The limiting softness is reached in the case of unimolecular, regular star polymers [7]. These *ultrasoft* colloids have recently attracted a lot of interest due to their unique architecture and interaction potential [8].

Soft in this context has two meanings: either the *single* particle itself is soft, which means that its molecular shape can be deformed very easily, or *many* particles interact via a soft, i.e. a long ranged, potential. So we have to distinguish between *intra*particle and *inter*particle softness. Some of the aforementioned examples such as micelles are even soft in both meanings. The total softness of such a system is governed by a complex interplay of the two contributions.

All soft colloids are extremely sensitive to the application of external shear fields [9]. To understand in detail the relation between softness and shear-induced structure there is an immense need for a soft colloidal model system. Such a model system should fulfil several criteria; the most important are (i) easy availability and (ii) precise and reproducible control of softness. A perfect situation would have in addition (iii) the possibility of controlling *intra*particle and *inter*particle softness independently to allow investigation of their individual contributions to the total softness of the particles.

We now want to introduce kinetically frozen micelles formed by the amphiphilic diblock copolymer poly(ethylene-alt-propylene)–poly(ethylene oxide), PEP–PEO, as a new *tunable* model system for soft colloids. The micellization behaviour of PEP–PEO was studied systematically by means of small angle neutron scattering (SANS) [10, 11] and is given schematically in figure 1. The characteristic properties of this system can be summarized as follows:

(i) In aqueous solution PEP–PEO forms micelles in which the hydrophobic PEP constitutes the insoluble core and the hydrophilic PEO the micellar corona (or shell). The aggregation numbers, P, of these micelles are unusually large due to the high interfacial tension, γ, of PEP against water. These properties lead to micellization even in a very asymmetric composition with high PEO content (star-like regime).

(ii) Although chemically not linked, exchange of diblock copolymers (the 'unimers') between different micelles could not be observed, even at elevated temperatures (the exchange kinetics of PEP–PEO micelles was studied by time-resolved SANS experiments [13]). It can therefore be concluded that the micelles are kinetically frozen.

(iii) The micellar properties can be tuned by changing the interfacial tension. This was accomplished by addition of a selective cosolvent, *N*,*N*-dimethylformamide (DMF) [14].

We will show that the softness of these micelles can be smoothly 'tuned' over an extremely broad range from nearly hard sphere-like to ultrasoft (star-like). This is valid for *single*-particle as well as for *many*-particle properties (interactions), which can be deduced from analysis of the (single-) particle form factor, $P(Q)$, and (many-) particle structure factor, $S(Q)$. Both quantities can be obtained from small angle neutron scattering (SANS) combined with contrast variation techniques [10, 15].

The paper is organized as follows. In section 2 all details concerning polymer synthesis and characterization as well as (Rheo-) SANS experiments and data analysis are given. In section 3 the results obtained will be presented and discussed starting with equilibrium, single-particle properties, i.e. the architecture of individual micelles (section 3.1). The interparticle properties, as obtained from analysis of the structure factor, $S(Q)$, in terms of an effective potential, are given in section 3.2. The first results of *in situ* shear experiments are given in section 3.3. Finally, in section 4 we give some conclusions and an outlook for future experiments.

2. Experimental details

2.1. Synthesis

The polymers used in this study were prepared by anionic polymerization [16]. The individual blocks of both polymers have been selectively protonated (h) or deuterated (d). The two isotopes have different coherent scattering lengths, $b_h = -3.74 \times 10^{-13}$ cm, $b_d = 6.67 \times 10^{-13}$ cm, so h/d labelling allows us to apply contrast variation in our SANS experiments; for details see section 3. The syntheses of the two block copolymers, h-PEP4-dh-PEO4 and h-PEP1-dh-PEO20,[2] were accomplished by a two-step process since the preparation of 1,4-polyisoprene, the parent material of PEP, requires reaction conditions different from those necessary for the anionic polymerization of ethylene oxide. The first step involves the polymerization of isoprene-h_8 with t-butyllithium as initiator and benzene as solvent. The living polymers were end capped by the addition of an excess amount of EO–h_4 and were terminated with acetic acid to obtain the fully protonated precursor polymers h-PI1-OH and h-PI4-OH. The hydroxy terminated poly(isoprenes) were subsequently saturated with hydrogen by means of a conventional Pd/$BaSO_4$ catalyst, resulting in the corresponding h-PEP1-OH and h-PEP4-OH polymers. In the second step of the synthesis the PEP-OH polymers were converted into the macro-initiators, h-PEP1-OK and h-PEP4-OK, by titration with naphthalene potassium in THF. The macro-initiators were used to polymerize mixtures of deuterated (CDN-Isotopes, Quebec, Canada, 99.8% D) and protonated ethylene oxide in THF at 50 °C for two days. After termination with a small amount of acetic acid the block copolymers were precipitated at −20 °C in acetone and finally freeze dried from benzene. A detailed characterization of the polymers was performed by gel permeation chromatography (GPC), ^{1}H and ^{13}C NMR; results are summarized in table 1. A more detailed description of the synthesis of PEP–PEO block copolymers was published earlier [17].

[2] The number denotes the nominal molar weight, M_w, in kg mol^{-1}.

Table 1. Molecular characteristics of PEP–PEO diblock copolymers.

Polymer	$M_{n,\mathrm{PEP}}$[a] (g mol^{-1})	$d_{p,\mathrm{PEP}}$[b]	$M_{n,\mathrm{PEO}}$[c] (g mol^{-1})	$d_{p,\mathrm{PEO}}$[b]	M_w/M_n[d]	$\Phi_{d-\mathrm{PEO}}$[e]
h-PEP4-dh-PEO4	4100	59	5 700	120	1.02	0.81
h-PEP1-dh-PEO20	1100	16	20 700	435	1.02	0.89

[a] ^{1}H NMR.
[b] Degree of polymerization.
[c] Calculated.
[d] Overall polydispersity from GPC.
[e] Volume fraction deuterated EO.

2.2. SANS

SANS experiments were performed using the KWS2 instrument at Forschungszentrum Jülich (FZJ), Jülich (Germany). These were followed by a series of measurements using D11 at the Institute Laue-Langevin (ILL), Grenoble (France), and PAXY at the Laboratoire Leon Brillouin (LLB), Saclay (France). Rheo-SANS experiments were performed using the SANS1 instrument at the Paul-Scherrer-Institut (PSI), Villigen (Switzerland).

SANS intensity raw data were corrected for contributions arising from the empty cell, solvent and incoherent background. They were finally normalized to an absolute scale (cm^{-1}) by the use of secondary standards such as Lupolen, water and plexiglass. This allows a comparison of data collected with different instruments. For details concerning the experimental technique, see for example [15].

Generally, the coherent macroscopic scattering cross-section measured in a SANS experiment has the following form:

$$\left(\frac{\mathrm{d}\Sigma}{\mathrm{d}\Omega}(Q)\right) = N_z\langle|A(Q)|^2\rangle \tag{1}$$

where N_z denotes the number density of scatterers and $A(Q)$ the scattering amplitude. Assuming that the critical micelle concentration is low, N_z can be approximated by

$$N_z = \frac{\phi N_\mathrm{A}}{P V_\mathrm{w}} \tag{2}$$

with ϕ the polymer volume fraction, P the aggregation number, V_w the weight average molar volume and N_A the Avogadro number. For a micellar structure consisting of a segregated PEP core and a PEO corona we can model the scattering amplitude by a spherical core–shell model [10, 11]:

$$A(Q) = P V_\mathrm{PEP}(\rho_\mathrm{PEP} - \rho_0)A(Q)_\mathrm{c} + P V_\mathrm{PEO}(\rho_\mathrm{PEO} - \rho_0)A(Q)_\mathrm{sh}. \tag{3}$$

Here $V_\mathrm{PEP} = V_{\mathrm{w,PEP}}/N_\mathrm{A}$ and $V_\mathrm{PEO} = V_{\mathrm{w,PEO}}/N_\mathrm{A}$ are the block volumes of an individual polymer chain and $A(Q)_\mathrm{c}$ and $A(Q)_\mathrm{sh}$ the scattering amplitudes of the core and shell, respectively. ρ_PEP and ρ_PEO denote the scattering length densities of PEP and PEO, respectively, and ρ_0 the scattering length density of the solvent. The scattering length densities are calculated using

$$\rho_j = \frac{\sum b_i}{v_j} \tag{4}$$

with j the individual component PEP monomer, PEO monomer or solvent molecule, $\sum b_i$ the sum of the coherent scattering lengths of all atoms in component j and v_j the average volume of one molecule of component j:

$$v_j = \frac{M_j}{d_j N_\mathrm{A}}. \tag{5}$$

M_j is the molar mass of the component j and d_j its corresponding density. $\rho_{\mathrm{h-PEP}}$ was calculated to be -3.05×10^9 cm^{-2}. For PEO, scattering length densities of 6.79×10^9 cm^{-2} for fully protonated and 7.52×10^{10} cm^{-2} for fully deuterated polymer were calculated. v_{PEP} was determined from the measured density of PEP1-OH at 20 °C, $d_{\mathrm{PEP}} = 0.850$ g cm^{-3}, and v_{PEPO} from $d_{\mathrm{PEO}} = 1.201$ g cm^{-3} [14]. For all partially deuterated materials the nominal degree of deuteration was considered for the calculations.

The partial scattering amplitudes, $A(Q)_{\mathrm{c,sh}}$, for the core and shell in spherical symmetry can be written as the Fourier transform of the radial density distribution, $n(r)$ [11]:

$$A(Q)_{\mathrm{c,sh}} = \frac{1}{C}\int_0^\infty 4\pi r^2 n(r)\frac{\sin(Qr)}{Qr}\,\mathrm{d}r. \tag{6}$$

In this equation $C = \int_0^\infty n(r)4\pi r^2\,\mathrm{d}r$ is a normalization constant.

For the micellar core we assumed for both diblock copolymers a constant density profile, $n(r) = 1$. This leads to

$$A(Q)_{\mathrm{c}} = \frac{3(\sin(QR_{\mathrm{c}}) - QR_{\mathrm{c}}\cos(QR_{\mathrm{c}}))}{(QR_{\mathrm{c}})^2}. \tag{7}$$

Here R_{c} denotes the core radius given by

$$R_{\mathrm{c}} = (3PV_{\mathrm{PEP}}/(4\pi))^{1/3} \tag{8}$$

assuming a compact solvent- and PEO-free core containing only PEP chains with a total volume PV_{PEP}.

For the micellar shell, on the other hand, a hyperbolic density distribution, r^{-x}, was taken. The density profile was convoluted with a Fermi function that serves as a cut-off function taking into account the finite chain length:

$$n(r) = \frac{r^{-x}}{1 + \exp((r - R_{\mathrm{m}})/(\sigma_{\mathrm{m}}R_{\mathrm{m}}))} \tag{9}$$

with R_{m} the overall micelle radius and σ_{m} the corresponding smearing parameter. x is a general power law exponent which in the case of constant density takes the value 0 (used for h-PEP4-dh-PEO4) and 4/3 for star-like structures (used for h-PEP1-dh-PEO20) [11]. Finally, we applied the convolution with the instrumental resolution function as given by Pedersen *et al* [18].

2.3. Shear experiments

Shear experiments were performed with a Couette-type shear cell, where the inner cylinder rotates. The shear cell is made of niobium—to be transparent to neutrons; a detailed description of the set-up is given in [19]. We used gap widths of $d = 0.5$ and 1.0 mm, respectively, and measured in a radial configuration, i.e. monitoring the flow–vorticity plane with the two-dimensional detector. The shear rate $\dot{\gamma}$ is defined by

$$\dot{\gamma} = \frac{v}{d} \tag{10}$$

with v the velocity at the outer radius and d the gap width. The shear cell can be operated with a maximum speed of 2000 rpm; therefore we were able to measure shear rates up to 3250 and 6500 s^{-1} with the two gap widths.

3. Results and discussion

To show the versatility of PEP–PEO micelles as a tunable model system for soft colloids, we have investigated two diblock copolymers, which should form the two extreme limits of possible micellar architectures. The first one is a symmetric diblock copolymer labelled h-PEP4-dh-PEO4, which we expect to form spherical micelles in aqueous solution [11, 12]. This block composition should guarantee a high aggregation number, that results in a micellar architecture similar to those of the usually used hard sphere model systems such as sterically stabilized poly(methyl methacrylate) latexes [20]. The opposite limit, i.e. a star-like architecture, can be achieved by an extremely asymmetric diblock copolymer labelled h-PEP1-dh-PEO20. We should emphasize that even for such a small hydrophobic block, which contains only 16 repeat units, a micelle is formed in aqueous solution. This arises from the extremely high interfacial tension between PEP and water, $\gamma = 46.0$ mN m^{-1}, as the driving force of micellization [14].

Taking advantage of contrast variation by labelling the hydrophobic PEP core oppositely to the hydrophilic PEO shell we were able to derive the molecular parameters of the different parts of an individual micelle by means of SANS. This was done by applying either shell contrast, i.e. matching the scattering length density of the PEP core by using appropriate isotopic solvent mixtures of H_2O and D_2O ($\rho_{\text{core}} = \rho_0$), or the core contrast, i.e. matching the scattering length density of the shell ($\rho_{\text{shell}} = \rho_0$). At low concentration we thus had direct access to partial shell or core form factors, $P(Q)$. To derive the pure intermicellar structure factor, $S(Q)$, without distortions from a concentration dependent micellar form factor, $P(Q)$, all concentrated solutions were investigated in core contrast solely. For guaranteeing good data quality even at high Q-vectors, we therefore choose the PEP core to be completely protonated. Using this labelling we were able to make measurements in deuterated solvents, which reduces the incoherent background substantially. Because the scattering length density of deuterated PEO is higher than that of D_2O the PEO blocks are partially deuterated, such that exact contrast matching of the shell could be achieved.

In the following we will discuss intraparticle and interparticle properties separately, starting with the micellar architecture obtained from the form factor, $P(Q)$, measured in dilute solutions.

3.1. Micellar architecture

For approaching the limit of infinite dilution, $P(Q, \phi = 0)$, a concentration series starting from a volume fraction $\phi = 10^{-2}$ has been investigated for both diblock copolymers. Micellar solutions of lower ϕ were prepared by dilution of the mother solution for $\phi \leqslant \phi^*$; solutions with higher concentrations had to be prepared individually directly in the SANS cells. In addition, we cross-checked the aggregation number of micellar solutions, which had been prepared individually. In all cases the same P was obtained. We should emphasize that the kinetical freezing of the micelles takes place upon dissolution; the precursor diblock copolymer melt is in equilibrium.

The lowest accessible volume fraction was $\phi = 5 \times 10^{-4}$ for h-PEP4-dh-PEO4 and $\phi = 10^{-3}$ for h-PEP1-dh-PEO20, although the intensity was only slightly above the background level, in particular at high Q-vectors. Figure 2 shows the partial form factor normalized to the volume fraction, $I(Q)/\phi$, in shell and core contrast for h-PEP4-dh-PEO4. Already, a qualitative discussion of the data reveals important features of the micellar architecture. First, the forward scatterings, $I(Q = 0)$, in the two contrasts are the same. This is expected for micelles formed by a symmetric diblock copolymer in shell and core contrast (we should note

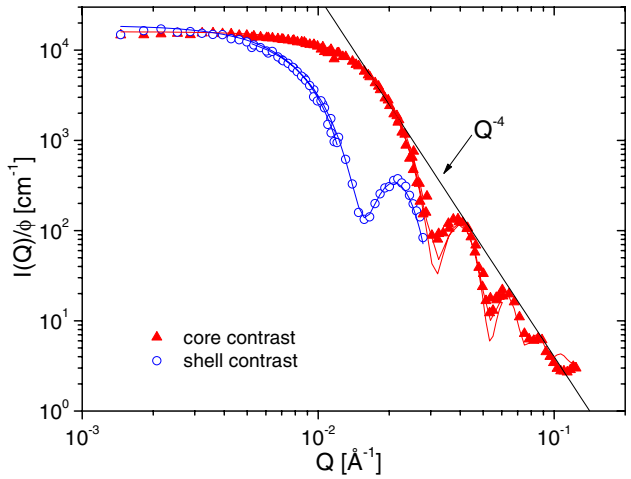

Figure 2. Form factor $P(Q)$ versus scattering vector Q for micelles formed by h-PEP4-dh-PEO4 in water; open symbols—shell and closed symbols—core contrast.

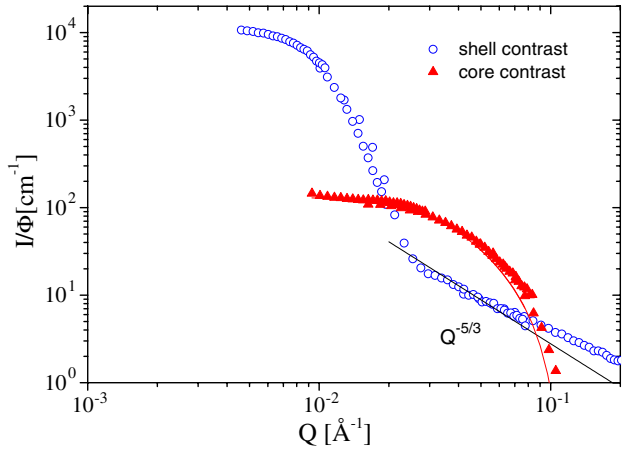

Figure 3. Form factor $P(Q)$ versus scattering vector Q for micelles formed by h-PEP1-dh-PEO20 in water; open symbols—shell and closed symbols—core contrast.

that the two blocks have the same molar volume V_w) and is in this sense a proof of the applied contrast conditions. This means that the scattering profiles shown in figure 2 are directly reflecting pure shell and core properties. Second, both scattering profiles show well defined maxima and minima, up to 4 in core contrast, which arise from sharp interfaces typical for a monodisperse, compact particle. Also shown is Porod's law $I \sim Q^{-4}$, which describes the limiting envelope of all form factor oscillations. (We should note that one has to consider that these oscillations are already smeared by the instrumental resolution function, so the data shown offer even more confirmation of the strong segregation between the core and corona and the low polydispersity of the micelles.) We should emphasize that in core contrast no *blob* scattering is visible [21, 22]. This also corroborates the compact PEP core. A quantitative analysis in terms of a core–shell model as described in section 2.2 gave the following micellar parameters: aggregation number $P = 1600$, core radius $R_{core} = 145$ Å and shell radius $R_m = 280$ Å with a polydispersity of ≈5%. The solvent fraction in the swollen shell is $\phi_{solv} = 60\%$.

Figure 3 shows the corresponding partial form factor data, $P(Q)/\phi$, in shell and core contrast for h-PEP1-dh-PEO20. The differences compared to figure 2 are obvious: the difference in forward scattering of the two contrasts is reflecting the asymmetry of the diblock

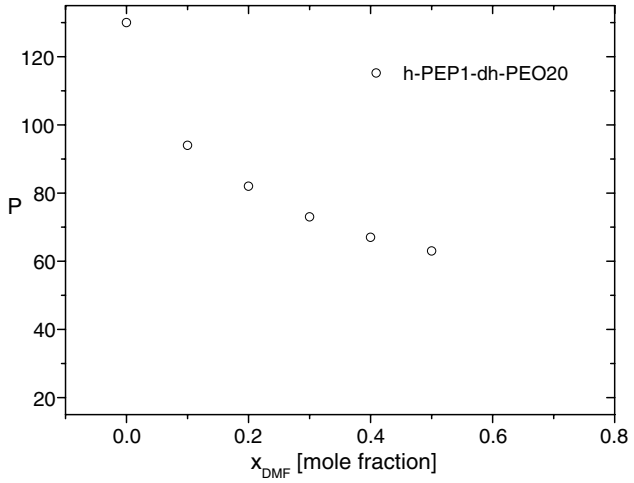

Figure 4. Aggregation number P versus DMF content for micelles formed by h-PEP1-dh-PEO20.

copolymer. Moreover, no maxima or minima are visible (also not at high Q in core contrast) and the power law observed in shell contrast has a slope of only $I \sim Q^{-5/3}$, which is typical for a polymer chain in a good solvent and arises from the swelling of the PEO in the shell (*blob* scattering). A quantitative analysis—see section 2.2—gives the following micellar parameters: aggregation number $P = 130$, core radius $R_{\text{core}} = 34$ Å and shell radius $R_{\text{m}} = 260$ Å.

If we assume the validity of the ultrasoft (star-like) interaction potential [8], equation (12), we see that for such a high aggregation number P (=functionality f) the potential is already very steep and close to a hard sphere potential. To increase the softness of our star-like micelles we have to decrease their aggregation number P. This was achieved by decreasing the interfacial tension, γ, between the hydrophobic PEP core and the solvent by the addition of a cosolvent, which is less incompatible with PEP. We chose *N*,*N*-dimethylformamide (DMF) as the cosolvent, $\gamma_{\text{DMF}} = 8.6\,\text{mN m}^{-1}$, and investigated the dependence of the aggregation number P on the DMF content in different water/DMF mixtures [14]. The data are shown in figure 4. By changing the interfacial tension γ we can 'fine-tune' the aggregation number/functionality of our star-like micelles from 130 for pure water to 63 for a water/DMF mixture with a DMF mole fraction $x_{\text{DMF}} = 0.5$. Therefore star-like micelles formed by h-PEP1-dh-PEO20 constitute an excellent 'tunable' model system for unimolecular star polymers.

3.2. Micellar interactions

For discussing in more detail the observed micellar interaction at higher volume fractions, it is recommended to refer directly to the structure factor $S(Q)$ rather than to the overall intensity $I(Q)$. $S(Q)$ is obtained assuming a decoupling between the form and structure factors [15].

Hard sphere-like interactions. Figure 5 shows the experimental structure factor $S(Q)$ for micelles formed by the symmetric diblock copolymer h-PEP4-dh-PEO4 in aqueous solution. $S(Q)$ was obtained by dividing the concentration dependent SANS intensity $I(Q, \phi)$ by the experimental form factor $P(Q) = I(Q, \phi = 0)$ shown in figure 2. All data can be simultaneously described using the Percus–Yevick structure factor for hard sphere systems [1], which results from the well known interaction potential

$$V(r) = \begin{cases} \infty & (r \leqslant R_{\text{HS}}); \\ 0 & (r > R_{\text{HS}}). \end{cases} \tag{11}$$

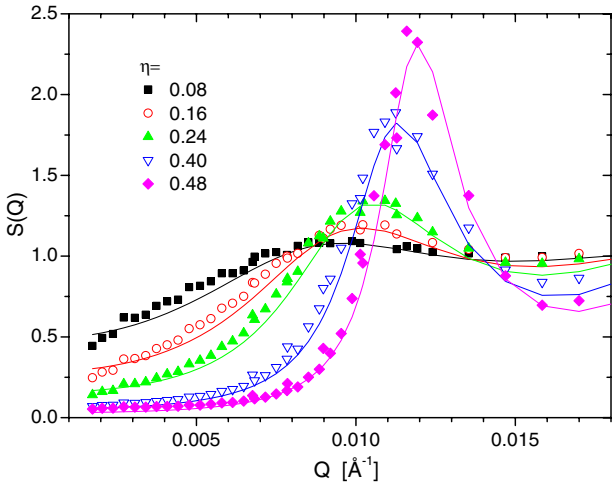

Figure 5. Structure factors $S(Q)$ versus scattering vector Q for micelles formed by h-PEP4-dh-PEO4 in water at different packing fractions η_{HS}. Solid curves: a Percus–Yevick fit; see the text.

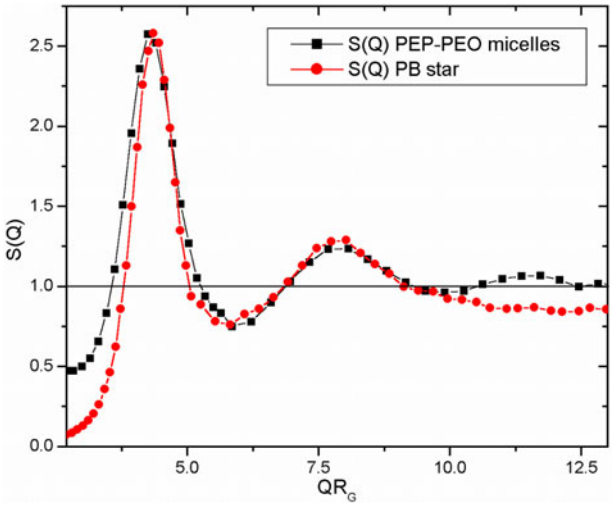

Figure 6. Structure factors $S(Q)$ versus the dimensionless axis QR for micelles formed by h-PEP1-dh-PEO20 in water/DMF(5:5) compared to $S(Q)$ obtained for unimolecular poly(butadiene) star polymers. The reduced volume fraction $\phi/\phi^* = 1$ for both systems; see the text.

Only one adjustable parameter is needed, that is the hard sphere diameter R_{HS}. We should emphasize that the concentrations are not adjustable parameters in our analysis. We take the aggregation number P to relate the number density of micelles N_z to the polymer volume fractions ϕ, $N_z = (\phi N_a)/(P V_{\mathrm{m}})$, and the hard sphere packing fraction $\eta = N_z \pi/6(2R_{\mathrm{HS}})^3$. The hard sphere radius $R_{\mathrm{HS}} = 290$ Å obtained from the fit is nearly identical to the micellar radius $R_{\mathrm{m}} = 280$ Å obtained from the form factor ($P(Q)$) analysis. This establishes the validity of hard sphere-like interactions between micelles formed by the diblock copolymer h-PEP4-dh-PEO4.

Ultrasoft (star-like) interactions. Figure 6 shows the experimental structure factor $S(Q)$ obtained for a micellar solution of the asymmetric diblock copolymer h-PEP1-dh-PEO20

in water/DMF with a DMF mole fraction $x_{\mathrm{DMF}} = 0.5$. For this solvent composition an aggregation number $P = 63$ was found. The micellar data are compared to the structure factor of a unimolecular 64-arm poly(butadiene) star polymer in d-methylcyclohexane [23]. Both systems are at their overlap volume fraction ϕ^*. Obviously the characteristic features of $S(Q)$ for the two systems are identical, in particular the peak height and the characteristic ratio of the peak positions.

A quantitative analysis of the star polymer SANS data as described in detail in [8] is applied—that is, starting from a pair potential $V(r)$ for star polymers which reads as follows:

$$\frac{V(r)}{k_{\mathrm{B}}T} = \begin{cases} (5/18)f^{3/2}[-\ln(r/\sigma) + (1+\sqrt{f}/2)^{-1}] & (r \leqslant \sigma); \\ (5/18)f^{3/2}(1+\sqrt{f}/2)^{-1}(\sigma/r)\exp[-\sqrt{f}(r-\sigma)/2\sigma] & (r > \sigma). \end{cases} \tag{12}$$

Here σ is the characteristic star size, i.e. the distance from the star centre to the centre of the outermost blob, and f the star functionality or arm number. Applying the Rogers–Young (RY) closure and associated Monte Carlo simulations we obtain information about the pair structure of the liquid, in particular the centre-to-centre structure factor $S(Q)$ of the stars. In attempting to fit the experimental data for the total scattering intensity $I(Q)$ with the theoretical predictions based on an analytic pair potential, we have to consider the fact that the star size itself has a dependence on the concentration. Whereas in the previous study [8] this could be done using experimental data for $\sigma(\phi)$, in the present study we have to use σ as (the only) adjustable parameter. The results of this quantitative analysis will be the subject of a forthcoming publication [24]. The excellent agreement between the data on the star polymer and star-like micelles confirms the applicability of star-like micelles as an analogue for unimolecular star polymers at high concentrations also. We should emphasize that the range of accessible functionalities fits perfectly to the most interesting region in the theoretical star polymer phase diagram recently calculated by Watzlawek *et al* [25], where a re-entrant melting is expected. Therefore our star-like micelles are a good starting point for verifying experimentally the predicted phase transitions.

We now want to elaborate in more detail the analogy of ultrasoft (star-like) colloids to the well known charge-stabilized colloids, but point out at the same time the substantial differences between the two systems. The analogy results from the use of a Yukawa-type potential for large star–star separations; see equation (12). The Yukawa potential was originally used for the description of interactions in solutions of charge-stabilized colloids. Here it reads as follows [1]:

$$V(r) = U_0 \frac{\exp(-\kappa r)}{r} \tag{13}$$

with an prefactor U_0 and an inverse screening length κ given by

$$\kappa^2 = \frac{(4\pi e^2)}{(\epsilon k_b T)}(Z^*\rho + 2\rho_{\mathrm{s}}). \tag{14}$$

In the case of high salt concentrations, i.e. when $\rho \gg \rho_{\mathrm{s}}$, κ depends only on the salt concentration. If we try to define a corresponding inverse screening length κ' from the Yukawa part in the star potential we arrive at

$$\kappa'^2 = \frac{f}{4\sigma^2}. \tag{15}$$

This means that the screening for star polymers is always governed by two parameters, namely the star size σ and star functionality f. Moreover, for ultrasoft (star-like) colloids such as our micelles we can in addition vary the *intra*particle softness, i.e. the molecular architecture of an individual micelle, which is not feasible for charge-stabilized colloids, where only the *inter*particle softness, in terms of the particle interactions, can be varied.

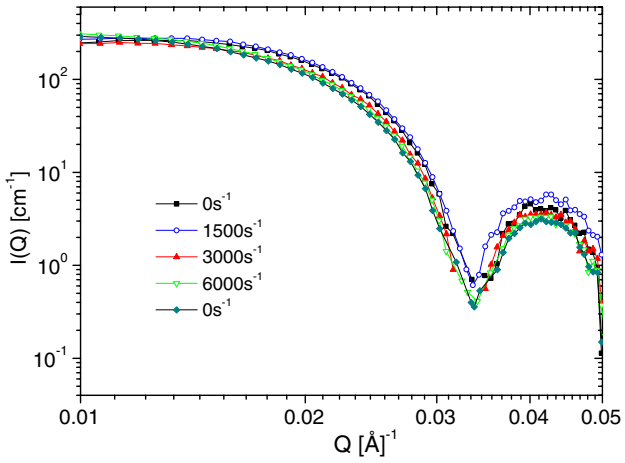

Figure 7. Intensity $I(Q)$ versus scattering vector Q for a dilute solution of micelles formed by h-PEP4-dh-PEO4 in water at different shear rates $\dot{\gamma}$.

3.3. Shear experiments

Theoretical predictions concerning the non-equilibrium phase diagram of charge-stabilized colloids under the influence of external shear should be transferable to our star-like micelles. Robins *et al* predicted a shear dependent re-entrant solidification in certain regions of the non-equilibrium phase diagram [26, 27]. We expect to observe an interesting interplay between this non-equilibrium re-entrant solidification and the equilibrium re-entrant melting predicted for star polymers when we apply external shear. For this reason we performed first *in situ* shear experiments (Rheo-SANS) on dense solutions of our star-like micelles formed by the diblock copolymers h-PEP1-dh-PEO20. In addition, we also investigated hard sphere-like micelles formed by the diblock copolymers h-PEP4-dh-PEO4 in order to have the possibility of 'calibrating' our shear experiments against other hard sphere systems [28].

All Rheo-SANS experiments were performed using core contrast conditions to avoid distortions from a shear rate dependent micellar form factor. In all experiments we observed no shear-induced anisotropy on the 2D detector, so we discuss only azimuthally averaged data in the following. Figure 7 shows data obtained in a Rheo-SANS experiment on a dilute solution, $\phi = 0.01$, of hard sphere-like micelles formed by the diblock copolymer h-PEP4-dh-PEO4. We show the scattering profile $I(Q)$ versus Q at different shear rates $\dot{\gamma}$. Although the shear rate is increased up to a value of $\dot{\gamma} = 6500\ \mathrm{s}^{-1}$, only minor changes are visible. In particular, the position of the form factor minimum is conserved, which confirms a shear rate independent core form factor. Moreover, on returning to equilibrium, $\dot{\gamma} = 0$, we find the same intensity profile. This corroborates the high shear stability of these micelles.

The effect of shear at higher volume fraction, $\phi = 0.1$, which corresponds to a hard sphere packing fraction $\eta_{\mathrm{HS}} = 0.4$, is shown in figure 8. We show the scattering profile $I(Q)$ versus Q at different shear rates $\dot{\gamma}$. The small changes visible in $I(Q)$ become clearer when we focus on the structure factor $S(Q) = I(Q)/P(Q)$, shown in figure 9. Up to a shear rate $\dot{\gamma} = 1300\ \mathrm{s}^{-1}$, the effect of external shear is to substantially decrease the peak height in $S(Q)$, which indicates a decrease of ordering in the micellar solution. Upon further increase of $\dot{\gamma}$ the peak height increases again, but the increase is much smaller than the initial decrease. This apparently non-linear behaviour of the peak height in $S(Q)$ needs to be investigated in more detail by further experiments. The peak position, on the other hand, which reflects the intermicellar distance, remains nearly unchanged for all $\dot{\gamma}$. Our results are comparable to experiments performed by Johnson *et al* [28] on solutions of sterically stabilized silica spheres.

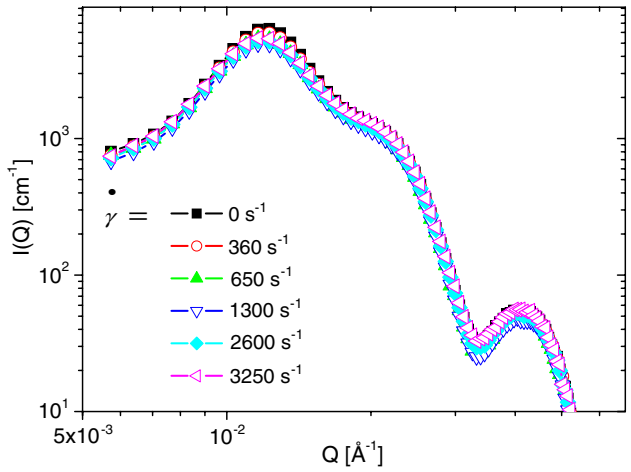

Figure 8. Intensity $I(Q)$ versus scattering vector Q for a concentrated solution of micelles formed by h-PEP4-dh-PEO4 in water at different shear rates $\dot{\gamma}$.

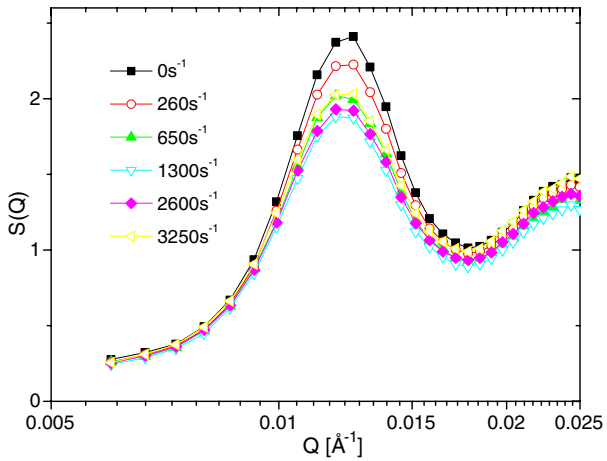

Figure 9. Structure factor $S(Q)$ versus scattering vector Q for a concentrated solution of micelles formed by h-PEP4-dh-PEO4 in water at different shear rates $\dot{\gamma}$.

These authors found qualitatively the same effects and analysed their data using theories of Ronis [29] and Dhont [30]. So we can conclude that our micelles behave as hard spheres under the influence of an external shear also.

As shown in figure 10, solutions of star-like micelles formed by the diblock copolymer h-PEP1-dh-PEO20 are more sensitive to the application of external shear. The volume fraction here is $\phi = 0.04$, which is already close to the overlap volume fraction ϕ^*. For this system a huge response to the shear field is already obvious at low shear rates. The peak in $I(Q)$ becomes more and more pronounced; i.e. an increase of order is observed with increasing shear rate. At the same time, the peak position shifts to lower Q-vectors, indicating a change in intermicellar distance. This effect is observed with increasing shear rate up to a value of $\dot{\gamma} = 5200\ \mathrm{s}^{-1}$. Further increase of $\dot{\gamma}$ has no effect; i.e. a high shear level is reached. Unfortunately, we had until now no data for the shear rate dependence of the form factor of our star-like micelles due to the extremely low intensity in core contrast. Thus we cannot derive the structure factor at the moment, but this is the most urgent future work that we have to do—also for verifying the shear stability of these micelles.

To summarize, for star-like micelles the shear effect is opposite to and much more pronounced than that observed for hard sphere-like micelles. This can be explained by use

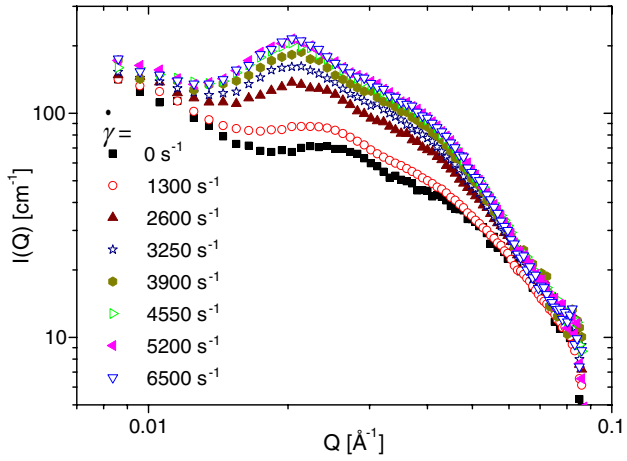

Figure 10. Intensity $I(Q)$ versus scattering vector Q for micelles formed by h-PEP1-dh-PEO20 in water at different shear rates $\dot{\gamma}$.

of the Deborah number, $D_e = \dot{\gamma}\tau_c$, an important dimensionless quantity for every shear experiment. Here τ_c is the characteristic relaxation time of the particles. For $D_e < 1$ the particles have enough time to relax within the timescale of the shear field, whereas for $D_e > 1$ the external perturbation is too fast. τ_c can be estimated in two ways. The first possibility is to use the time needed to diffuse over a typical interparticle distance a: $\tau_c = a^2/(6D_0)$. From the peak position Q_m in $S(Q, \phi)$ we obtain a; we estimate D_0 by use of the Stokes–Einstein equation. For both systems, a has a value of ≈100 Å. From this estimate we obtain values of $\dot{\gamma} \approx 10^4$ for reaching $D_e = 1$, a value that is far from experimentally accessible shear rates. The second possibility is to define τ_c as the time needed to diffuse over its own radial distance R, $\tau_c = R^2/(6D_s(\phi))$, with $D_s(\phi)$ the self-diffusion coefficient at volume fraction ϕ, which we can estimate by replacing the solvent viscosity η_0 by the solution viscosity $\eta(\phi)$ in the Stokes–Einstein equation. The viscosity of the micellar solution of h-PEP4-dh-PEO4 investigated is ≈10 cP, whereas that for h-PEP1-dh-PEO20 is already ≈200 cP (this solution is already close to its overlap volume fraction). This means that, although the micelles formed by h-PEP1-dh-PEO20 are slightly smaller (as also is their interparticle distance) and the volume fraction is smaller, the larger viscosity dominates, so larger Deborah numbers are already reached at smaller shear rates. We need $\dot{\gamma} \approx 5 \times 10^3$ to be at $D_e = 1$ for the hard sphere system h-PEP4-dh-PEO4, whereas for the star-like micelles formed by h-PEP1-dh-PEO20 only a value of $\dot{\gamma} \approx 4 \times 10^2$ is needed. This is reflected in the observed pronounced shear sensitivity of the star-like micelles, which therefore constitute an interesting starting point for future shear experiments.

4. Conclusions

The specific micellization behaviour as well as the easy availability of block copolymers with the desired molar weight and composition make the PEP–PEO/water/DMF system a nearly ideal colloidal model system. In particular, in the star-like regime, use of the micelles provides an elegant way to overcome the immense effort requirement and synthesis problems inherent to unimolecular star polymers. The main advantage of our PEP–PEO system, when compared to other diblock copolymers, e.g. polystyrene–polyisoprene (PS–PI)[5] and poly(ethylene oxide)–polypropylene–poly(ethylene oxide) (PEO–PPO–PEO) [31], 'Pluronics', is the high interfacial tension of PEP in water. This results in (i) a high kinetic stability and (ii) the capability of really achieving the star-like regime.

The micellar interaction potential can be adjusted between the two limits of hard sphere-like, i.e. short ranged repulsive, and ultrasoft (=star-like), i.e. long ranged repulsive, as shown by the structure factors presented, obtained by means of SANS. All intermediate potentials are expected to be achievable just by changing the diblock copolymer composition and/or interfacial tension. Therefore this system may be seen as an electrically neutral analogue of the well known charge-stabilized colloids, where the interaction length, i.e. the 'softness' of the potential, can be adjusted by changing the salt concentration.

Acknowledgments

We acknowledge W Pyckhout-Hintzen (FZJ), J Kohlbrecher (PSI), K Mortensen (Risoe), P Lindner (ILL) and L Noirez (LLB) for their assistance during the SANS experiments and the corresponding neutron scattering facilities for allocation of beam time. We acknowledge financial support by the Deutsche Forschungsgemeinschaft (DFG) in the framework of the Transregio Sonderforschungsbereich TR6 (Teilprojekt A2).

References

[1] Pusey P N 1991 *Liquids, Freezing and the Glass Transition* ed J P Hansen, D Levesque and J Zinn-Justin (Amsterdam: Elsevier)
[2] Royall C P, Leunissen M E and van Blaaderen A 2003 *J. Phys.: Condens. Matter* **15** S3581
[3] Dhont J K G, Lettinga M P, Dogic Z, Lenstra T A J, Wang H, Rathgeber S, Carletto P, Willner L, Frielinghaus H and Lindner P 2003 *Faraday Discuss.* **123** 157
[4] Vermant J, Raynaud L, Mewis J, Ernst N and Fuller G G 1999 *J. Colloid Interface Sci.* **211** 221
[5] McConnel G A, Lin M Y and Gast A 1995 *Macromolecules* **28** 6754
[6] Dhont J K G, Gompper G and Richter D (ed) 2002 *Matter and Materials* vol 10 *Soft Matter: Complex Materials on Mesoscopic Scale* (Jülich: Schriften des Forschungszentrums Jülich)
[7] Grest G S, Fetters L J, Huang J S and Richter D 1996 *Adv. Chem. Phys.* **94** 67
[8] Likos C N, Watzlawek M, Löwen H, Abbas A, Jucknischke O, Allgaier J and Richter D 1998 *Phys. Rev. Lett.* **80** 4450
[9] Löwen H 2001 *J. Phys.: Condens. Matter* **13** R415
[10] Poppe A, Willner L, Allgaier J, Stellbrink J and Richter D 1997 *Macromolecules* **30** 7462
[11] Willner L, Poppe A, Allgaier J, Monkenbusch M, Lindner P and Richter D 2000 *Europhys. Lett.* **51** 628
[12] Kaya H, Willner L, Allgaier J, Stellbrink J and Richter D 2002 *Appl. Phys.* A **74** (Suppl.) 499
[13] Willner L, Poppe A, Allgaier J, Monkenbusch M and Richter D 2001 *Europhys. Lett.* **55** 667
[14] Lund R, Willner L, Stellbrink J, Radulescu A and Richter D 2003 *Macromolecules* submitted
[15] Higgins J S and Benoit H C 1994 *Polymers and Neutron Scattering* (Oxford: Oxford University Press)
[16] Hsieh H L and Quirk R P 1994 *Anionic Polymerisation* (New York: Dekker)
[17] Allgaier J, Poppe A, Willner L and Richter D 1997 *Macromolecules* **30** 1582
[18] Pedersen J S, Posselt D and Mortensen K 1990 *J. Appl. Crystallogr.* **23** 321
[19] Mortensen K, Almdal K, Bates F S, Koppi K, Tirrell M and Norden B 1995 *Physica* B **213/214** 682
[20] Pusey P N and van Megen W 1986 *Nature* **320** 340
[21] Dozier W D, Huang J S and Fetters L J 1991 *Macromolecules* **24** 2810
[22] Svaneborg C and Pedersen J S 2002 *Macromolecules* **235** 1028
[23] Stellbrink J, Allgaier J, Monkenbusch M, Richter D, Lang A, Likos C N, Watzlawek M, Löwen H, Ehlers G and Schleger P 2000 *Prog. Colloid Polym. Sci.* **115** 88
[24] Laurati M, Stellbrink J, Lund R, Willner L, Richter D and Zaccharelli E 2004 *Phys. Rev. Letters* at press
[25] Watzlawek M, Likos C N and Löwen H 1999 *Phys. Rev. Lett.* **82** 5289
[26] Stevens M J, Robbins M O and Belak J F 1991 *Phys. Rev. Lett.* **66** 3004
[27] Stevens M J and Robbins M O 1993 *Phys. Rev.* E **48** 3778
[28] Johnson S J, de Kruif C G and May R P 1988 *J. Chem. Phys.* **89** 5909
[29] Ronis D 1984 *Phys. Rev.* A **29** 1453
[30] Dhont J K G 1989 *J. Fluid Mech.* **204** 421
[31] Mortensen K, Brown W and Norden B 1992 *Phys. Rev. Lett.* **68** 2340